International Conference on Mathematics, Computational Methods & Reactor Physics (M&C 2009)
Saratoga Springs, New York, May 3-7, 2009, on CD-ROM, American Nuclear Society, LaGrange Park, IL (2009)

ANALYTICAL DESCRIPTION OF PULSES MEASURED WITH AN ORGANIC LIQUID SCINTILLATOR FOR PULSE SHAPE DISCRIMINATION

S. D. Ambers, M. Flaska, S. A. Pozzi
University of Michigan, Department of Nuclear Engineering and Radiological Sciences, Ann Arbor, Michigan, USA
sambers@umich.edu; mflaska@umich.edu; pozzisa@umich.edu

ABSTRACT

In this paper, we present a new pulse shape discrimination (PSD) approach that is based on detailed knowledge of the detector response to given radiation. Traditionally, PSD has been performed using the standard methods such as charge-integration method. Average pulses were obtained for multiple pulse height regions separately for neutrons and gamma rays. The average neutron and gamma-ray pulses were implemented into the new PSD algorithm for classification of a large number of measured pulses. This new PSD approach proves to be more accurate than the standard charge-integration PSD method for low-energy neutron and gamma rays under 90 keVee (keV electron equivalent). The improvement is greater than a factor of two for neutrons in the smallest pulse height bin considered, which was from 26 to 35 keVee. For this pulse height bin, which corresponds to a total energy deposited by the neutron with energy between 200 and 260 keV, approximately 72% of the neutrons were correctly classified.

Key Words: liquid scintillator, pulse shape discrimination, average neutron and gamma-ray pulses

1. INTRODUCTION

Neutron and gamma-ray pulse shape discrimination (PSD) using organic scintillation detectors is a widely adopted method in fields such as nuclear nonproliferation, international safeguards, nuclear material control and accountability, and national security. In contrast to thermal neutron detectors such as He-3 tubes, organic scintillators are able to detect high-energy neutrons and do not need to use moderating material. At the same time, these detectors are sensitive to gamma-rays, which makes them very suitable for measurements in mixed neutron/gamma-ray fields. A large number of papers were published on PSD performance of liquid scintillators [1-5]. In this paper, we present a new PSD approach that is based on detailed knowledge of the performance of a detector to a given radiation. Specifically, an average detector response is obtained for several energies, which is later used as a 'reference' for particle identification. The main objective of this work was to find out if there is potential for further improvement of the PSD performance with the existing measurement setup.

2. PULSE SHAPE DISCRIMINATION METHOD

For the work described here, the CAEN V1720, 12-bit, 250-MHz digitizer was used to store a few million pulses directly from the anode of the liquid scintillator EJ-309. The detector is 13.3-cm high with a diameter of 13 cm. A 1-μCi Cs-137 source was placed on the face of the detector as a source of gamma rays. This provided a large number of known gamma-ray pulses. Since full-energy deposition does not occur in the liquid EJ-309 the recorded pulses covered a full range of energies corresponding to the amount of energy lost by the gamma rays inside of the liquid due to Compton scatterings. In order to acquire known neutron pulses the time of flight (TOF) method was implemented using a 20-μCi Cf-252 spontaneous fission source. The TOF experiment was done by placing the Cf-252 source on the face of a liquid EJ-309 detector which acted as the start detector. Fig.1 shows the measurement configuration. The liquid scintillation detector of the same type and size was as the start detector was placed 30 cm from the source and was used as the stop detector. Only this detector was used for the acquisition of neutron pulses.

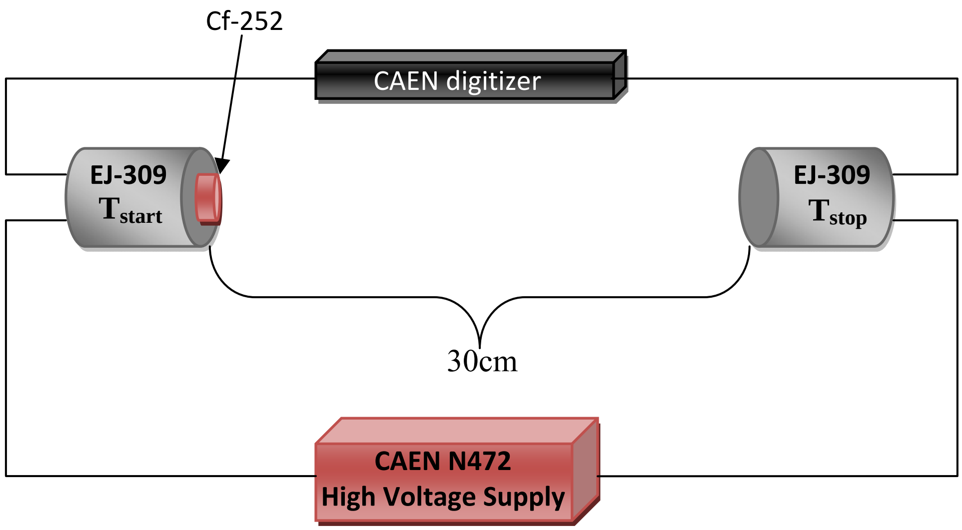

Figure 1. TOF Measurement Setup

To accomplish the TOF measurement with the CAEN digitizer, the stop detector initiated a local trigger, which in turn initiated a global trigger for both detectors. Whenever a global trigger was sent to the start detector a waveform was saved from the buffer even if no interaction occurred. This ensured that the pulses from both detectors were correlated in time. It was important to use the same detector with the same gain for both the neutron and gamma-ray measurements to properly determine the detector response. No shielding was used between the source and either of the detectors. The total time window for the measured pulses was set to 604 ns to ensure the full tail of the pulse would be included for optimal performance of the charge-integration PSD method so a comparison of the two methods could be performed.

As the first step, the TOF for each measured pulse was calculated using a MATLAB® post-processing script. The script calculated the time differences between the start and stop pulses using the time values at 20% of the pulses maxima. The delta T results are plotted as a histogram in Fig.2.

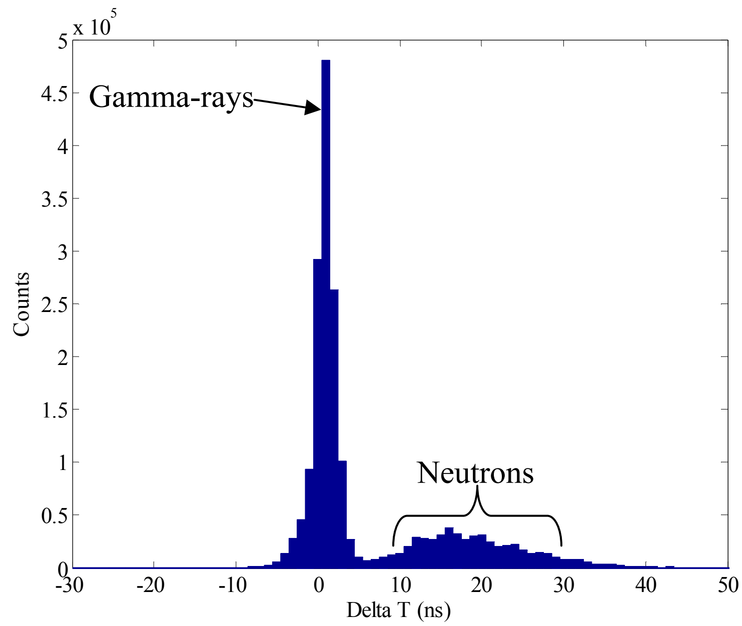

Figure 2. Measured time-of-flight distribution from a Cf-252source.

Neutron pulses were recorded by enforcing the condition that the time difference values are in the region between 10 and30 ns (see Fig. 2). The number of accidental pulses was determined in the region from -30 to -10 ns and the ratio of accidental to neutron pulses was found to be approximately 1:72.

Once neutron pulses were collected, both the neutron and gamma-ray pulses were run through a cleaning algorithm in order to discard any clipped or pulses with multiple peaks. Next, the pulses were binned by pulse height into 19 bins. The binning was done such that more bins were created at low energies, where there is a higher concentration of pulses. For each pulse height bin, a single 'typical' pulse was obtained by averaging all the pulses within the bin. This step was done separately for neutrons and gamma rays. Thus, thirty eight average pulses were obtained in total. Four of the neutron and four of the gamma-ray average pulses are shown in Fig. 3. The pulses were normalized to their maximum values to allow for comparison.

Fig. 3 shows the well-known behavior of neutrons and gamma rays in liquid scintillators, which results in a difference in the fraction of light in the tail of the pulses. While the shape of the gamma-ray pulses does not significantly change with energy deposited (i.e., pulse height), the shape of the neutron pulses is highly dependent on the energy deposited.

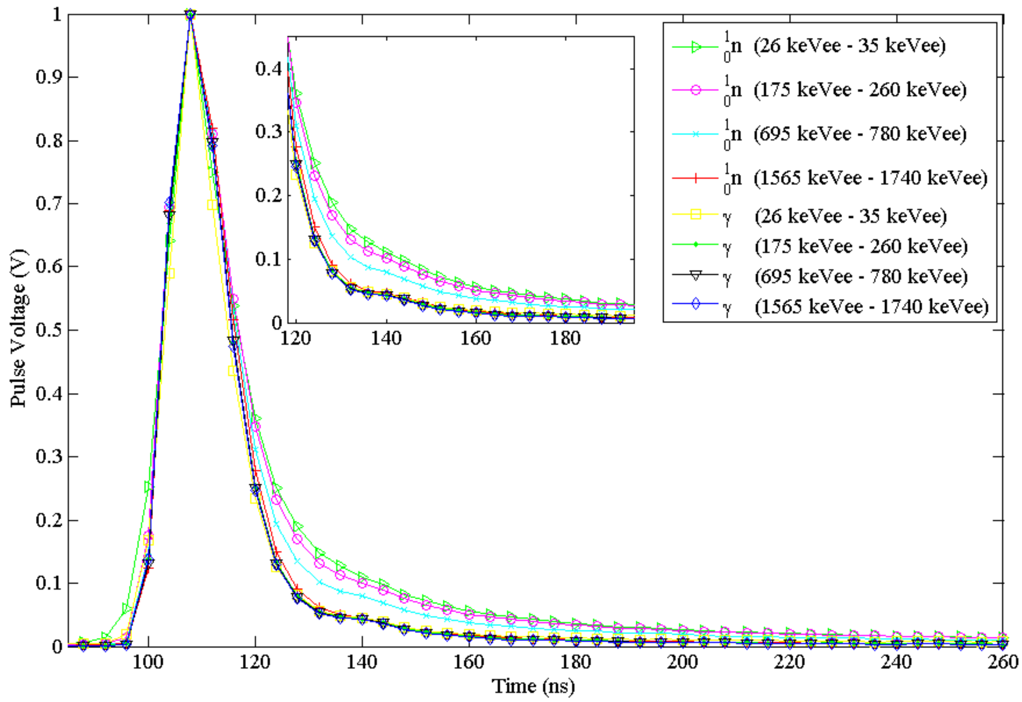

Figure 3. Normalized average neutron and gamma-ray pulses (zoomed in view of the tails are inset to emphasize the differences). Large differences are observed between neutron pulses themselves and neutron and gamma-ray pulses.

The acquired average pulses were then used as a reference for identifying and distinguishing neutrons from gamma rays measured with the EJ-309. Specifically, each measured pulse is compared point by point to the average neutron and gamma-ray pulses with the appropriate pulse height. The comparison is done in the tail region of the pulse where the difference is the most prevalent. The average pulses and the 'unknown' measured pulses are normalized in order to compare the pulse shapes regardless of the bin width. Each pulse is then identified by determining the smallest sum of absolute differences between the average pulses and the unknown pulse as a neutron or gamma ray.

The average-pulses PSD method was compared to the standard charge-integration method by post-processing the same set of measured known TOF neutrons and known Cs-137 gamma rays with both methods and examining the results. For the standard method, an optimized offline digital PSD method was used [6]. This method is based on a standard charge-integration method [7, 8] which calculates the integral ratio of two different pulse intervals. Typically, the first interval covers the tail of a pulse, while the second interval covers the total pulse interval. Generally, the heavier the particle is the larger fraction of light is in the tail of the pulse. This results in a larger ratio of tail-to-total-integrals for neutrons when compared to gamma rays [9, 10]. The integration range was optimized for the best separation of neutron and gamma-ray pulses when the tail integral is plotted against the total integral. The neutrons have a larger tail integral since the scintillation light takes longer to be emitted through the de-excitation of the scintillation molecule after interacting with a neutron than a gamma ray. The charge-integration method is not accurate at discriminating neutrons and gamma rays at low energies. Fig. 4 shows two PSD results at two different thresholds.

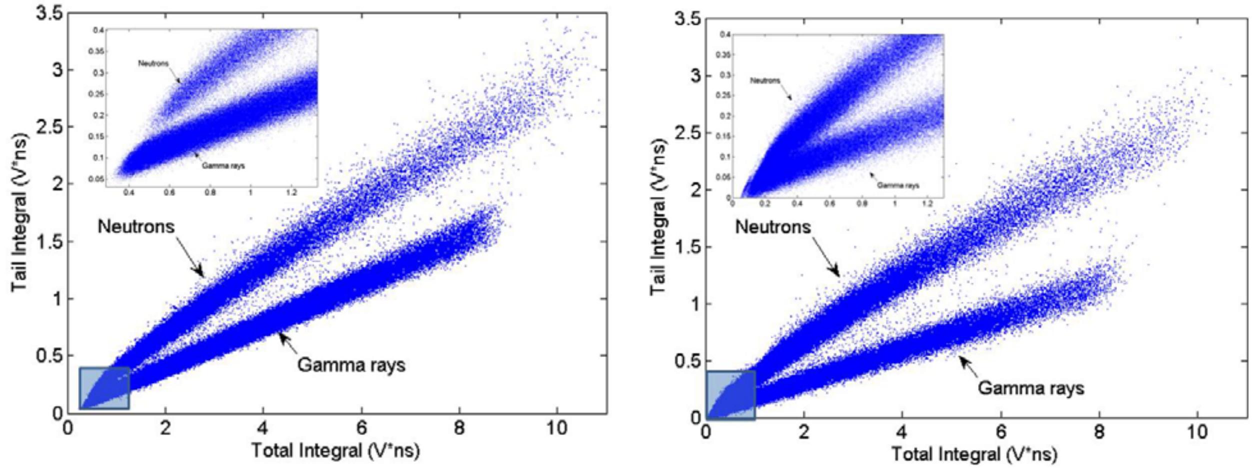

(a) (b)

Figure 4. Tail integral versus total integral for (a) 70 keVee threshold, (b): 26 keVee (200 keV neutron energy) threshold. Standard charge-integration PSD method was used.

From the inset of Fig.4a very good separation can be seen between the neutrons and the gamma rays for a measurement threshold of 70 keVee (490 keV neutron energy deposited). In Fig. 4b the separation between the neutron and gamma rays is poor for small total integral values, as the threshold is lowered to 26 keVee (200 keV neutron energy deposited). This lack of separation at lower energies makes it very difficult to discriminate between neutron and gamma-ray pulses. This is the region where the average-pulses PSD method could improve pulse identification.

3. RESULTS

3.1. Pulse Shape Discrimination Using Average Pulses

Approximately 2.5 million TOF neutron pulses were processed by a MATLAB® algorithm that calculated the sum of absolute differences between the measured and average pulses. At low energies, the pulses were significantly affected by noise. This noise makes comparing of the average pulses difficult. The average pulses appear smooth when plotted because the noise is random and disappears when averaged over thousands of pulses. Once the absolute differences were found between the average and measured pulses the sums of the differences were compared and the pulse was identified by the smaller of the two sums. Fig. 5 shows a plot of a measured neutron pulse with both the neutron and gamma-ray average pulses.

The inset of Fig. 5 shows the range in which the sum of absolute difference is calculated for each pulse. This range was chosen because it is the region which shows the difference between average neutron and gamma-ray pulses.

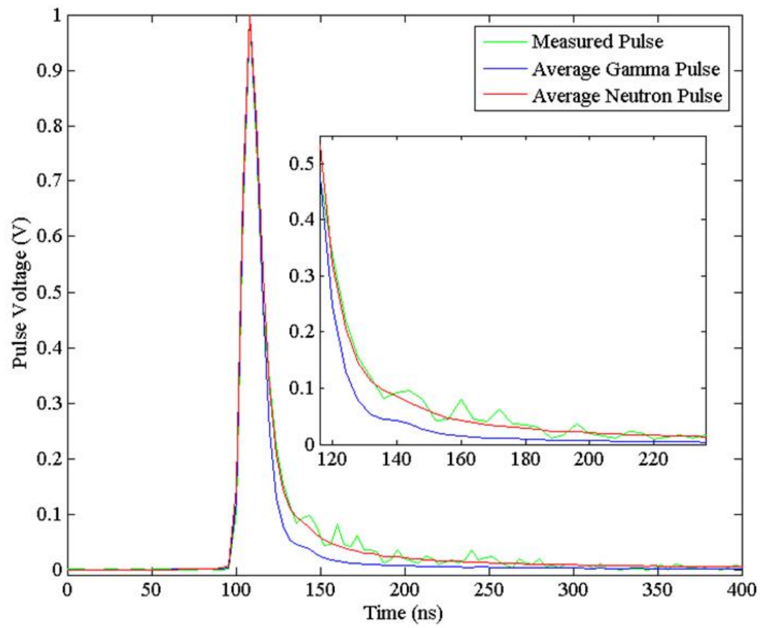

Figure 5. Illustration of the average-pulses PSD method. Measured neutron pulse with average neutron and gamma-ray pulses are shown.

The measured neutron pulse shows smaller absolute difference when compared to the average neutron pulse and therefore the average pulse PSD method identified it correctly as a neutron.

3.2. Pulse Shape Discrimination Using Charge-Integration Method

The standard charge-integration method was applied to both the TOF neutrons and the Cs-137 gamma rays. This method performed very well with the gamma-ray pulses. The method was able to successfully identify 99% of the Cs-137 gamma rays above 26 keVee. This is because the gamma rays maintain the same slope when viewed on a plot of the tail to total integrals as seen in Fig. 6. On the other hand, as the neutrons decrease in energy their slope changes. This low-energy slope change results in a region where the neutron and gamma-ray pulses overlap. This region has been outlined in yellow in Fig. 6. This overlap region is where the charge-integration method incorrectly classifies low-energy neutrons as low-energy gamma rays.

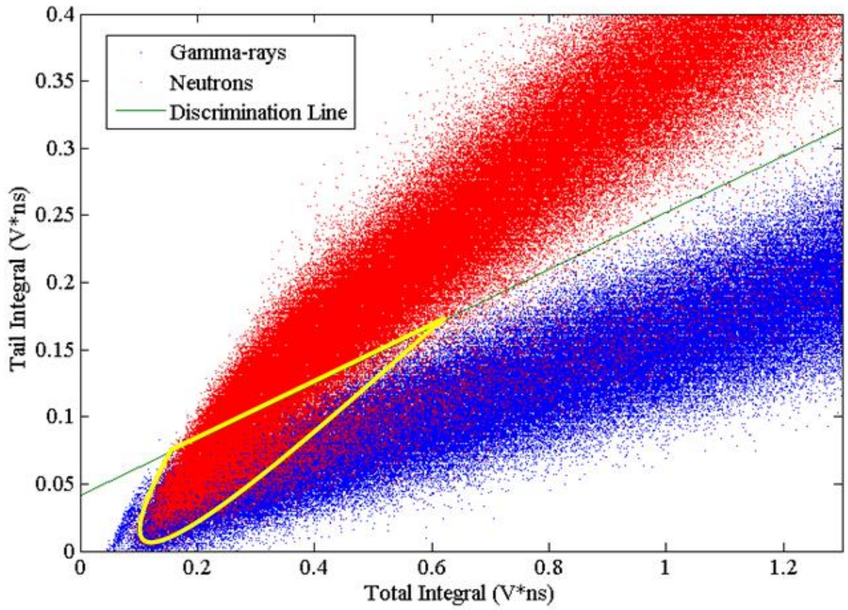

Figure 6. Time-of-flight attributed neutron and gamma-ray pulses illustrate the shortcoming of the charge-integration method for small pulses (overlap region shown with the yellow marker).

3.3. Comparison of the Two PSD Methods

The two methods were analyzed by determining the percentage of correctly identified pulses. This was done by running the TOF-attributed neutrons and Cs-137 gamma rays through each PSD algorithm and recording the number of classified neutrons and gamma rays. Results for the smallest four energy bins along with the total energy range can be seen in Tables I and II.

Table I. Average-Pulses PSD Method: TOF Neutron Results. Percentage of correctly classified neutrons is given in the highlighted column.

Bins (keVee)	Total # Pulses	# Neutrons	% Neutrons	# Gammas	% Gammas
26-35	131,831	95,449	72.40	36,382	27.60
35-43	149,240	113,564	76.09	35,676	23.91
43-65	346,130	278,704	80.52	67,426	19.48
65-87	281,261	239,670	85.21	41,591	14.79
26-1,738	2,647,693	2,322,374	87.71	325,319	12.29

Table II. Charge-Integration PSD Method: TOF Neutron Results. Percentage of correctly classified neutrons is given in the highlighted column.

Bins (keVee)	Total # Pulses	# Neutrons	% Neutrons	# Gammas	% Gammas
26-35	131,831	40,388	30.64	91,443	69.36
35-43	149,240	62,369	41.79	86,871	58.21
43-65	346,130	203,661	58.84	142,469	41.16
65-87	281,261	216,618	77.02	64,643	22.98
26-1,738	2,647,693	2,156,846	81.46	490,847	18.54

The results given in Tables I and II show that the average-pulses PSD method improves the classification of the measured low-energy neutrons by a factor of approximately 2 when compared to the standard charge-integration method. The principal reason for this improvement is due to the overlap region seen in Fig. 6. The same analysis was performed on the Cs-137 pulses and both sets of findings are tabulated in Tables III and IV.

Table III. Average-Pulses PSD Method: Cs-137 Gamma-Ray Results. Percentage of correctly classified gamma rays is given in the highlighted column.

Bins (keVee)	Total # Pulses	# Neutrons	% Neutrons	# Gammas	% Gammas
26-35	122,711	14,712	11.99	107,999	88.01
35-43	108,567	10,958	10.09	97,609	89.91
43-65	235,041	17,701	7.53	217,340	92.47
65-87	205,261	11,144	5.43	194,117	94.57
26-1,738	3,930,090	168,602	4.29	3,761,488	95.71

Table IV. Charge-Integration PSD Method: Cs-137 Gamma-Ray Results. Percentage of correctly classified gamma rays is given in the highlighted column.

Bins (keVee)	Total # Pulses	# Neutrons	% Neutrons	# Gammas	% Gammas
26-35	122,711	562	0.46	122,149	99.54
35-43	108,567	475	0.44	108,092	99.56
43-65	235,041	854	0.36	234,187	99.64
65-87	205,261	497	0.24	204,764	99.76
26-1,738	3,930,090	3,561	0.09	3,926,529	99.91

The gamma-ray results show that the charge-integration method identifies 99.9% of the gamma rays correctly. This is because the gamma rays follow the slope of the discrimination line therefore they are always under the classification line. Although the average-pulses PSD method shows a lower percentage of correctly identified gamma rays than the integration method, it still correctly identified gamma-ray pulses 95% of the time.

4. CONCLUSIONS

Liquid scintillators are frequently used in conjunction with optimized PSD methods to accurately distinguish neutrons from gamma rays. The standard PSD method based on charge integration has excellent properties for liquid scintillators such as EJ-309. The method can be used to accurately discriminate neutrons from gamma rays originating from a neutron source. The new PSD method that is proposed in this paper is based on average neutron and gamma-ray pulses that serve as a reference for identifying the measured particles. This new method shows improved particle identification at low energies (200 keV neutron energy). This improvement will allow neutron identification at low energies when measured with a single EJ-309 liquid scintillator, because the need of using the TOF approach to identify low-energy neutrons is eliminated. An increased sensitivity for particle identification is beneficial in many fields of nuclear measurements such as nuclear nonproliferation, international safeguards, nuclear material control and accountability, and national security.

REFERENCES

1. B. Sabbah, A. Suhami. "An accurate pulse-shape discriminator for a wide range of energies," Nucl. Instr. and Meth. A 58 pp. 102-110 (1968).
2. J. Kalyna, I.J. Taylor. "Pulse shape discrimination: An investigation of n-γ discrimination with respect to size of liquid scintillator," Nucl. Instr. and Meth. A 88 pp. 277-287 (1970).
3. P. Sperr, H. Spieler, M.R. Maier, D. Evers. "A simple pulse-shape discrimination circuit," Nucl. Instr. and Meth. A 116 pp. 55-59 (1974).
4. J.A. Lockwood, C. Chen, L.A. Friling, D.Swartz, R.N. St. Onge, Aaron Galonsky, et al. "Response functions of organic scintillators to high energy neutrons," Nucl. Instr. and Meth. A 138 pp. 353-362 (1976).
5. J.M. Adams, G. White. "A versatile pulse shape discriminator for charged particle separation and its application to fast neutron time-of-flight spectroscopy," Nucl. Instr. and Meth. A 156 pp. 459-476 (1978).
6. M. Flaska, S.A. Pozzi. "Identification of shielded neutron sources with the liquid scintillator BC-501A using a digital pulse shape discrimination method," Nucl. Instr. and Meth. A 577, pp. 654-663 (2007).
7. D. Wolski, M. Moszynski, T. Ludziejewski, A. Johnson, W. Klamra, O. Skeppstedt. "Comparison of n-γ discrimination by zero-crossing and digital charge comparison methods," Nucl. Instr. and Meth. A 360 pp. 584-592 (1995).
8. H. Klein, S. Neumann. "Neutron and photon spectrometry with liquid scintillation detectors in mixed fields," Nucl. Instr. and Meth. A 476 pp. 132-142 (2002).
9. L.M. Bollinger, G.E. Thomas, Rev. Sci. Instrum. "Measurement of the Time Dependence of Scintillation Intensity by a Delayed-Coincidence Method," 32 pp. 1044 -1050 (1961).
10. J.B. Birks. "The Theory and Practice of Scintillation Counting," Pergamon Press, Oxford, pp. 219-227 (1964).